Supplementary Data for

# Eradication of large solid tumors by gene therapy with a T cell receptor targeting a single cancer-specific point mutation

Matthias Leisegang, Boris Engels, Karin Schreiber, Poh Yin Yew, Kazuma Kiyotani, Christian Idel, Ainhoa Arina, Jaikumar Duraiswamy, Ralph R. Weichselbaum, Wolfgang Uckert, Yusuke Nakamura and Hans Schreiber

*Index of Supplementary Data*

**Supplementary Methods**

*Whole-exome and RNA sequencing*

Genomic DNA and total RNA were extracted from the Bulk tumor cells using AllPrep DNA/RNA mini kit (Qiagen, Ventlo, The Netherlands) while genomic DNA of 20 original 8101 tumor fragments and Reis#1 and Reis#2 was extracted using QIAamp DNA Micro Kit (Qiagen). Whole-exome DNA libraries were prepared from 2-3 μg of genomic DNA using SureSeletXT Mouse All Exon V1 (Agilent Technologies, Santa Clara, CA). RNAseq libraries were prepared from 1 μg of total RNA using TruSeq Stranded Total RNA Library Prep kit (Illumina). The prepared whole-exome and RNAseq libraries were quantified on the 2200 Tape Station (Agilent Technologies), and then sequenced by 150 bp paired-end reads on NextSeq 500 Desktop Sequencer or HiSeq2500 Sequencer (Illumina).

*Variant calling*

Somatic variants (SNVs and indels) were called using a Fisher's exact test-based method with the following parameters (i) base quality ≥15, (ii) sequence depth ≥10, (iii) variant depth ≥4, (iv) variant frequency in tumor ≥10%, (v) variant frequency in normal <5%, and (vi) Fisher *P* value <0.05 (19). SNVs and indels were annotated using ANNOVAR (20) based on RefGene. To test intratumor heterogeneity, we merged variant data of all samples into a single file and made variant position lists, and then called variants at these positions using the following criteria: (i) base quality ≥15, (ii) sequence depth ≥50 in all samples, (iii) variant depth ≥2, (iii) variant frequency in normal 0%, (iv) Fisher *P* value <0.05. Hierarchical clustering analysis was performed using R statistical software version 3.1.1 (R Core Team, R Foundation for Statistical Computing, Vienna, Austria).

*TCR gene transfer*

Plat-E packaging cells were transiently transfected with MP71-1D9 or MP71-2C (22) by calcium phosphate precipitation. 48 h after transfection, virus supernatant was harvested, filtered and used for transduction. Spleens were isolated from OT-I-Rag$^{-/-}$ mice and erythrocytes were lysed by ammonium chloride treatment. Cells were incubated in RPMI (+ 10% FCS, 2 mM glutamine, 50 µM 2-mercaptoethanol, 1 mM HEPES, 1 mM sodium pyruvate, 1x non-essential amino acids, 100 U/ml penicillin, 100 µg/ml streptomycin, and 50 µg/ml gentamycin) supplemented with 6 U/ml human IL-2 (Roche, Basel, Switzerland) and 1 µM SIINFEKL peptide (provided by Steven Meredith) at a concentration of 4x10$^6$/ml. On the following day, spleen cells were transferred to RetroNectin-coated 6-well plates (12.5 µg/ml (TaKaRa, Otsu, Japan)) together with 3 ml virus supernatant (+ 4 µg/ml protamine sulfate (Sigma Aldrich, St. Louis, MO)) followed by spinoculation (800 x g, 90 min, 32 °C). Cells were used 48 or 72 h after transduction for adoptive transfer or *in vitro* assays, respectively.

*Longitudinal imaging*

Windows were implanted onto the shaved back of H-2K$^b$-positive or H-2K$^b$-negative Rag$^{-/-}$ mice. MC57-mp68-GFP or MC57-SIY-GFP cancer cells were injected at 3-5 different sites in between the fascia and dermis of the rear skin layer. Naive 1D9tg T cells were injected as described above. Erythrocytes of 150 µl blood were labeled using DiD (Life Technologies) as described (32) and injected *i.v.* on the day of T cell transfer. For *in vivo* imaging, anesthetized mice were positioned on a custom-made stage adaptor that held the window on the exact same position. A motorized microscope XY scanning stage and Leica LAS-AF software allowed recording individual 3-dimensional positions per field-of-view and returning to them later with high precision. Using blood vessels as “landmarks”, same vessels could be located within 50 µm when returning on the same day, or within 100 µm on the next day. Data were acquired using a Leica SP5 II TCS tandem scanner two-photon spectral confocal

microscope (long-working distance 20x/NA 0.45 and 4x/NA 0.16 dry lenses, Olympus). To determine the fraction of area occupied by fluorescent cells ($GFP^+$ cancer cells, DiD-labeled erythrocytes), acquired images were analyzed using Fiji software (Laboratory for Optical and Computational Instrumentation; University of Wisconsin-Madison, WI).

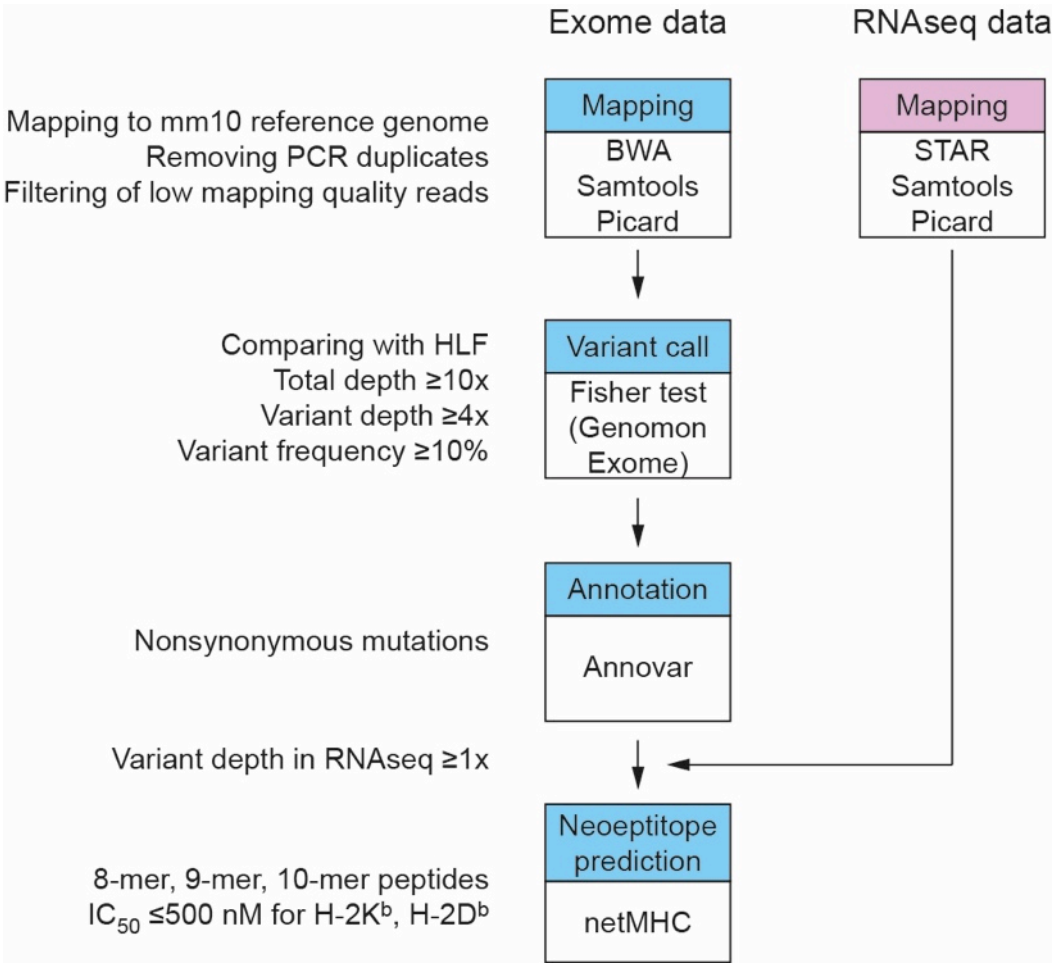


**Supplementary Fig. S1 - Pipeline for exome/RNA analysis and neoepitope prediction.**

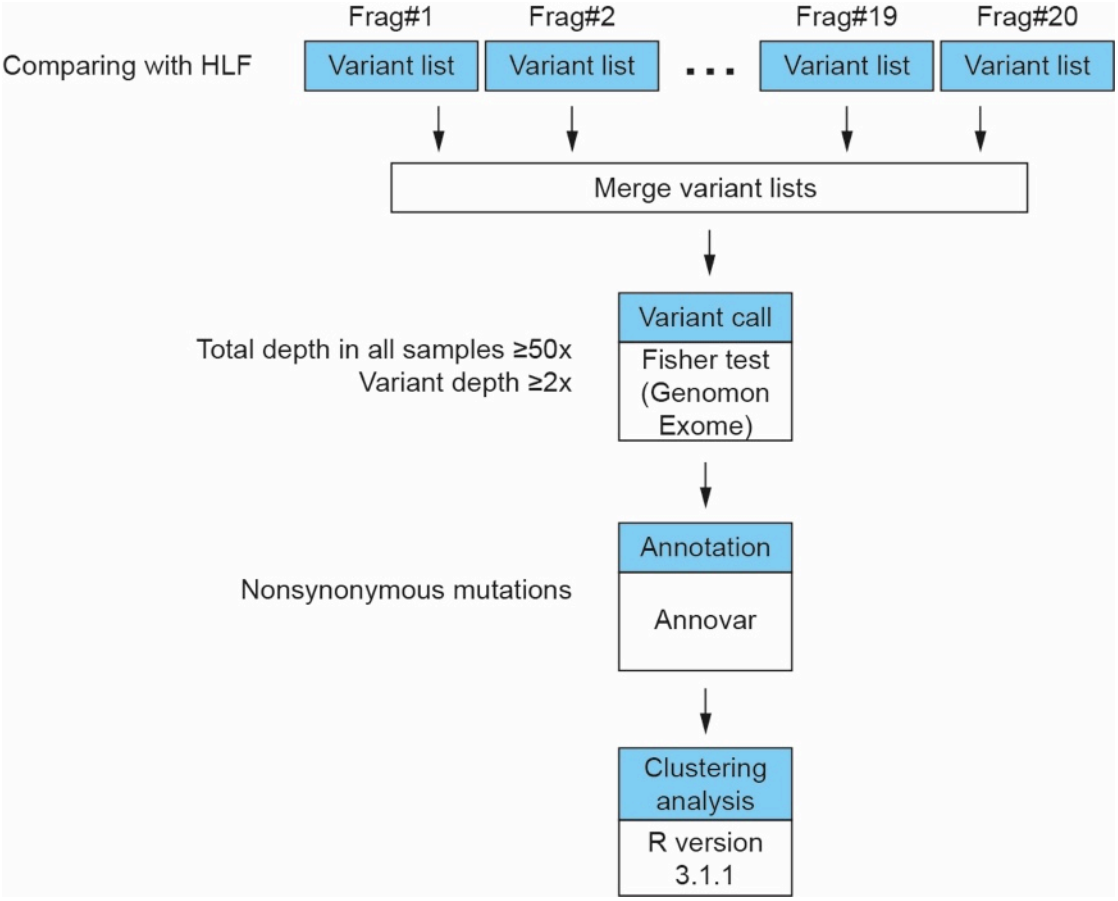


**Supplementary Fig. S2 - Pipeline for exome and clustering analysis of autochthonous 8101 tumor fragments.**

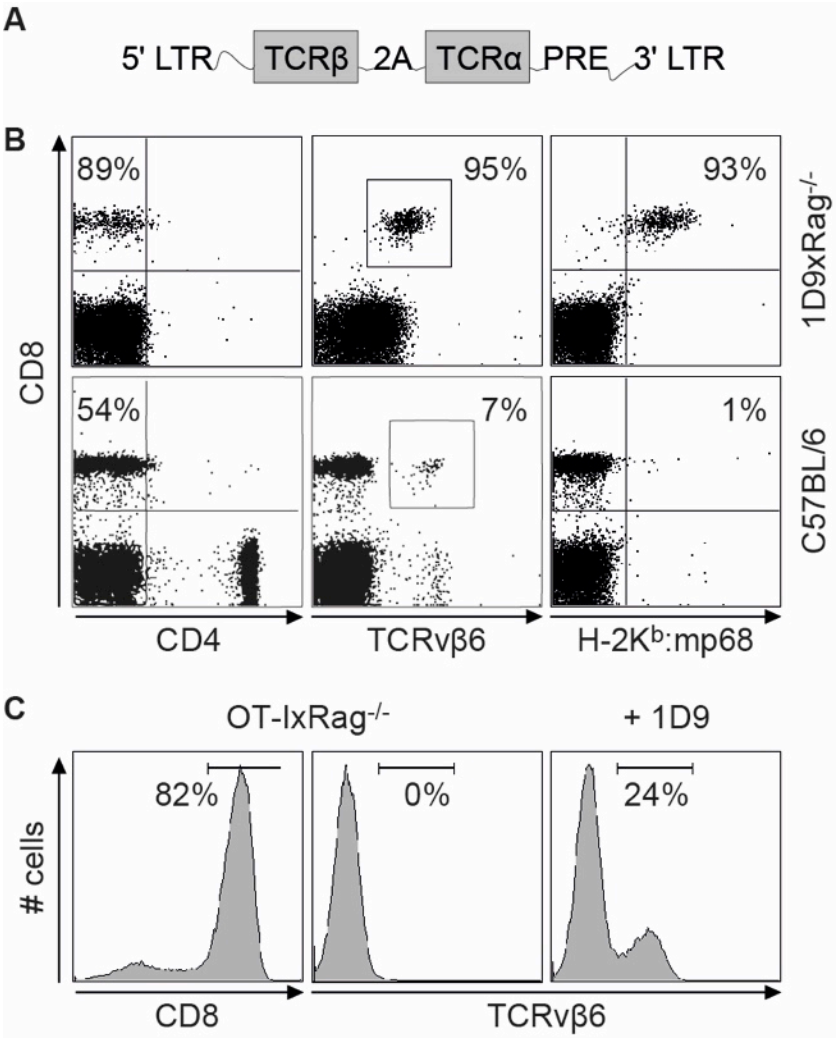


**Supplementary Fig. S3 - Generation of 1D9 T cells.** A, Schematic representation of the 1D9 retrovirus. The TCRα- and β-chain genes were introduced into the MP71-PRE retrovirus vector (see reference in (22)) linked by a 2A element. LTR: long terminal repeat of the mouse myeloproliferative sarcoma virus; 2A: 2A element of porcine teschovirus; PRE: post-transcriptional regulatory element of the woodchuck hepatitis virus. B, Representative staining of blood samples from 1D9xRag$^{-/-}$ and C57BL/6 mice. Left panels show staining for CD4 and CD8. Numbers indicate percentage of CD8$^{+}$ T cells of all lymphocytes. Expression of TCRvβ6 and the 1D9 TCR was detected using TCRvβ6-specific antibodies and H-2K$^{b}$:mp68 multimers, respectively. C, Cultured T cells derived from splenocytes of OT-IxRag$^{-/-}$ mice were analyzed for CD8 expression. 1D9 TCR expression was determined using TCRvβ6-specific antibodies before and after transduction with 1D9 retrovirus.

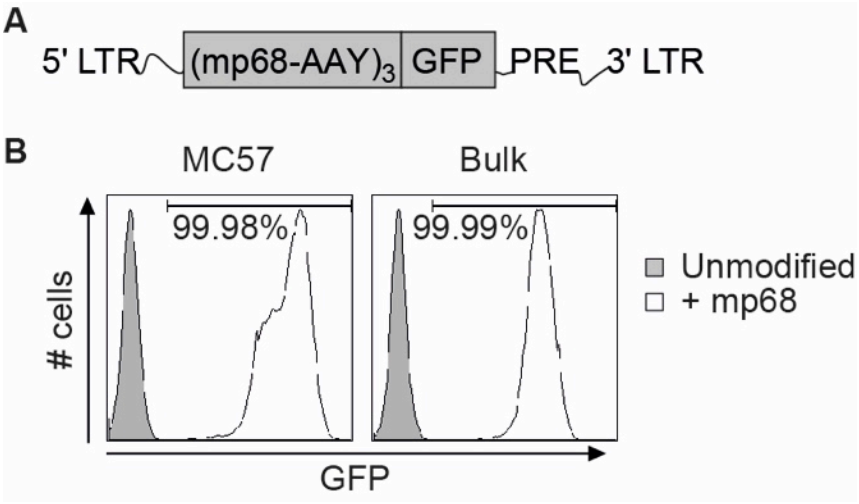


**Supplementary Fig. S4 - Generation of mp68-expressing tumor cell lines.** A, Scheme of the retrovirus encoding the trimeric minigene SNFVFAGI-AAY fused to GFP (mp68-GFP). LTR: long terminal repeat of the mouse myeloproliferative sarcoma virus; PRE: post-transcriptional regulatory element of the woodchuck hepatitis virus. B, Flow cytometric analysis of mp68-GFP fusion proteins expressed by the transduced and sorted tumor cells MC57 and Bulk. Parental MC57 and Bulk (unmodified, gray) were analyzed for comparison. Numbers indicate percentage of mp68-GFP-expressing cells.

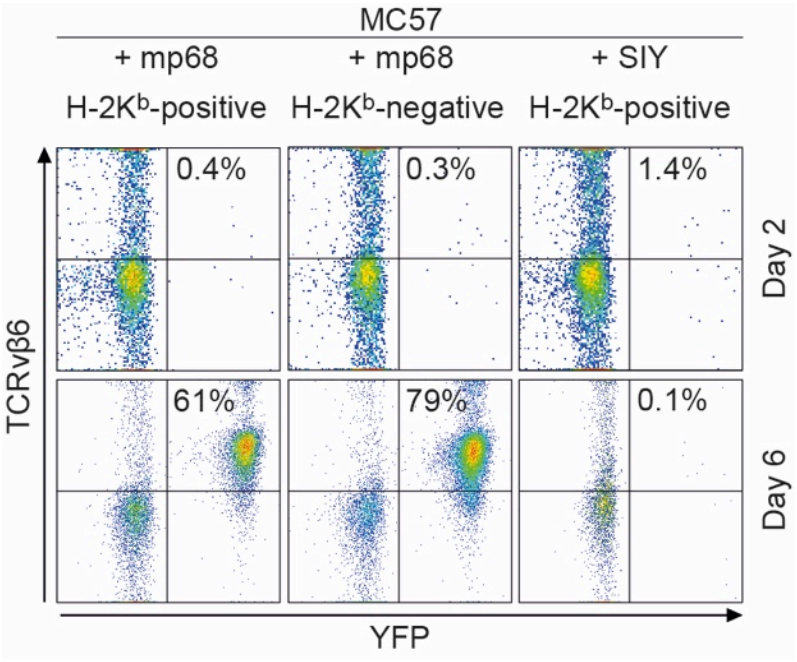


**Supplementary Fig. S5 - Expansion of 1D9 T cells is antigen-specific and not driven by lymphopenia-induced proliferation.** Splenocytes of YFPx1D9xRag$^{-/-}$ mice were transferred into H-2K$^{b}$-positive and H-2K$^{b}$-negative Rag$^{-/-}$ mice bearing MC57-mp68 or MC57-SIY tumors. 1D9 T cells were monitored in blood taken on day 2 and 6 after adoptive transfer. Numbers indicate the percentage of YFP$^{+}$/TCRvβ6$^{+}$ double-positive cells.

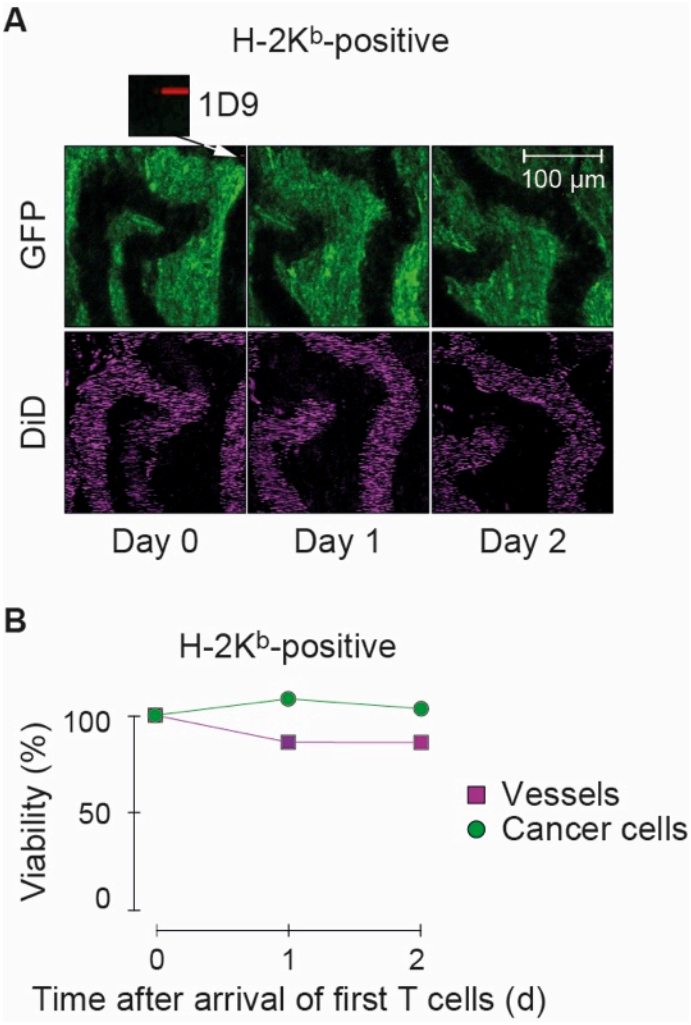


**Supplementary Fig. S6 - 1D9 T cells do not infiltrate tumors if mp68 is not expressed.** A, Longitudinal imaging of an established MC57-SIY tumor grown in a Rag$^{-/-}$ mouse following adoptive transfer of 1D9 T cells of YFPx1D9xRag$^{-/-}$ mice. Day 0 is the first day on which T cell infiltration was found in animals with MC57-mp68 tumors in the same experiment (see Fig. 4A, left). At that time point, one T cell (pseudo-colored in red, see magnification) was visible in the blood stream. Viability of tumor tissue was analyzed by monitoring GFP (cancer cells, green) and blood flow (DiD-stained erythrocytes, purple). B, Quantification of the areas shown in (A) that are covered by live cancer cells (green) and functional vessels (purple). Areas on day 0 were defined as 100%.

**Supplementary Table S1** - Results of whole exome sequencing of Bulk tumor cells and Bulk reisolates after 1D9 T cell therapy.

| | | | $p68^{S551F}$ | | | $p53^{S238A}$ | | |
|---|---|---|---|---|---|---|---|---|
| **Sample** | **Average depth** | **Nonsynonymous SNV** | **Wild type** | **Mutant** | **VAF (%)** | **Wild type** | **Mutant** | **VAF (%)** |
| **Heart-lung fibroblasts** | 158 | 0 | 207 | 0 | 0 | 56 | 0 | 0 |
| **Bulk** | 146 | 7,923 | 161 | 52 | 24 | 8 | 30 | 79 |
| **Reis#1** | 125 | 7,808 | 182 | 3 | 2 | 42 | 18 | 30 |
| **Reis#2** | 92 | 7,809 | 108 | 17 | 14 | 10 | 24 | 71 |

Reis: Reisolates
VAF: Variant allelic frequency

**Supplementary Table S2** - Results of whole exome sequencing of fragments derived from the autochthonous 8101 tumor.

| | | | p68$^{S551F}$ | | | p53$^{S238A}$ | | |
|---|---|---|---|---|---|---|---|---|
| **Sample** | **Average depth** | **Nonsynonymous SNV** | **Wild type** | **Mutant** | **VAF (%)** | **Wild type** | **Mutant** | **VAF (%)** |
| **Heart-lung fibroblasts** | 158 | 0 | 207 | 0 | 0 | 56 | 0 | 0 |
| **Frag#1** | 83 | 7,726 | 77 | 42 | 35 | 28 | 12 | 30 |
| **Frag#2** | 101 | 8,481 | 119 | 46 | 28 | 29 | 6 | 17 |
| **Frag#3** | 91 | 7,861 | 79 | 60 | 43 | 29 | 17 | 37 |
| **Frag#4** | 76 | 7,785 | 55 | 43 | 44 | 26 | 11 | 30 |
| **Frag#5** | 79 | 336 | 120 | 4 | 3 | 35 | 0 | 0 |
| **Frag#6** | 80 | 1,703 | 118 | 4 | 3 | 34 | 0 | 0 |
| **Frag#7** | 60 | 7,522 | 50 | 19 | 28 | 10 | 5 | 33 |
| **Frag#8** | 77 | 6,602 | 77 | 20 | 21 | 17 | 6 | 26 |
| **Frag#9** | 77 | 7,801 | 63 | 43 | 41 | 24 | 12 | 33 |
| **Frag#10** | 83 | 7,754 | 67 | 45 | 40 | 18 | 13 | 42 |
| **Frag#11** | 93 | 7,845 | 93 | 42 | 31 | 22 | 10 | 31 |
| **Frag#12** | 93 | 7,540 | 106 | 36 | 25 | 24 | 8 | 25 |
| **Frag#13** | 84 | 7,488 | 74 | 30 | 29 | 29 | 11 | 28 |
| **Frag#14** | 79 | 7,612 | 85 | 28 | 25 | 23 | 6 | 21 |
| **Frag#15** | 78 | 7,270 | 87 | 30 | 26 | 28 | 11 | 28 |
| **Frag#16** | 72 | 5,523 | 122 | 22 | 15 | 13 | 3 | 19 |
| **Frag#17** | 86 | 7,423 | 90 | 30 | 25 | 23 | 5 | 18 |
| **Frag#18** | 80 | 6,485 | 90 | 30 | 25 | 25 | 3 | 11 |
| **Frag#19** | 64 | 7,694 | 67 | 33 | 33 | 9 | 12 | 57 |
| **Frag#20** | 78 | 7,551 | 74 | 31 | 30 | 30 | 17 | 36 |

Frag: Fragment
VAF: Variant allelic frequency